# Feasible Operation Region-based Constraint Management of Distribution Networks with Soft Open Points

Xun Jiang, *Member, IEEE,* Yue Zhou, *Member, IEEE,* Jianzhong Wu, *Fellow, IEEE,* Wen long Ming, *Member, IEEE*

***Abstract*— Soft open points (SOPs) are power electronic devices placed at normally open points of electricity distribution networks. With millisecond-level control, SOPs are promising in constraint management of distribution networks facing the significant uncertainties from renewable power generation and customer behaviors (such as electric vehicle travelling behaviors). This paper develops a novel feasible operation region (FOR)-based method for optimal SOP control. The FOR, denoted as the allowable range of nodal power injections of distribution networks, can be used to replace the power flow equations and network constraints in a conventional optimal power flow (OPF)-based model. Due to the one-to-one correspondence between FOR boundaries and thermal/voltage constraints, FOR-based constraint management method can adapt to various measurement conditions. Moreover, the FOR constraints can be converted into a format based on line flows and node voltages, allowing for the use of real-time measurements of these operating parameters rather than the measurements of nodal power load/generation that are normally not accessible online. The proposed method is validated on the IEEE 33-node distribution network and IEEE 123-node distribution network. The performance of the method is also compared with that of conventional OPF-based control.**

***Index Terms*—Feasible operation region, soft open point, distribution network, constraint management, network observability.**

## I. Introduction

In the transition to net zero carbon emission, increasing low-carbon technologies such as renewable distributed generation (DG), energy storage systems and electrified demand like electric vehicles and heat pumps, are connected to electricity distribution networks. These technologies will greatly increase the total/peak power generation/load in distribution networks, bringing great challenges in network planning, design and operation.

Soft open points (SOPs) have proved to be an alternative to enhance the capability of the distribution network in integrating low-carbon technologies. SOPs are advanced power electronic devices placed at normally open points of electricity distribution networks. Through flexible power transfer and independent reactive power compensation, SOPs can improve the distribution of the power flows and the voltage profile across the networks. Since the provision of SOPs in 2007 by Siemens AG company in Germany, researchers have done studies on the benefit analysis of SOPs including feeder load balancing, network loss reduction, voltage profile improvement, hosting capacity enhancement, post-fault restoration, etc. [1], [2].

In studies on SOP control, optimal power flow (OPF) based methods that incorporate power flow equations are normally employed for optimal SOP control [3-6]. However, they require global information regarding power load and generation, which makes the OPF-based methods impractical given that the measurements across most distribution networks are not universally available [7]. Moreover, the complex global optimization might hinder the fast response of SOPs against the frequent power/voltage fluctuations in the networks [6]. To reduce the computational burden, sensitivity-based OPF methods can be used for SOP control [8], [9]. This method uses sensitivity analysis to assess the impact of SOP power adjustments on line currents or node voltages, eliminating the need for power flow equations. However, like conventional OPF methods, the sensitivity-based OPF methods also require complete observation of the load and generation conditions to continuously update the sensitivity coefficients [10].

In contrast, local control for SOPs can be easily implemented based on local information such as the measurements of the bus voltage at each port of SOPs [11]. Considering the respective advantages of OPF-based control and local control, one compromise is the decentralized control [11], [12], which is achieved based on local information of each area and boundary interaction among connected areas. In recent years, data-driven method is also used for achieving a near-global optimal SOP control strategy with only a few accessible measurements [13], [14]. For the data-driven method to remain adaptable, it requires historical/measurement data that covers various operational states of the distribution network. However, capturing representative network states is challenging, especially with the uncertainties from increasing generation/load. Additionally, network security issues and unreliable measurement data raise concerns among distribution network operators about relying on this method.

In this paper, we developed a novel SOP control method, leveraging the feasible operation region (FOR) methodology. The FOR methodology was first developed for assessing the steady-state security of electricity transmission networks [15],

This work was supported in part by China Scholarship Council and in part by the Engineering and Physical Sciences Research Council, U.K., through the UK/China MC2 project under Grant EP/T021969/1 and the Supergen Energy Networks Hub project under Grant EP/Y016114/1.

The authors are with Department of Electrical and Electronic Engineering, School of Engineering, Cardiff University, Cardiff, CF24 3AA, U.K. (e-mail: JiangX28, ZhouY68, WuJ5, MingW@cardiff.ac.uk).

[16] and has started to be applied to electricity distribution networks [17-19] in recent years. The main idea of the methodology is to obtain the range of operating states that satisfy both the power/load flow equations and the constraints imposed by equipment operating limits. By obtaining the FOR constraints analytically, the operators need only check if a given operating state lies within the obtained operation region, while avoiding solving the power flow equations [16], [20]. Furthermore, the FOR constraints can replace the network constraints and power flow equations in the optimization scheme [17], [18].

This paper exploits the FOR constraints in the formulation of the OPF model for optimal SOP control. The main contributions of the proposed method are as follows:

1) The original FOR constraints are converted into a new format based on line flows and node voltages. This enables the constraint management of the distribution network with SOPs using these operating parameters rather than nodal power load and generation that are normally not accessible online.

2) Compared to existing OPF methods which require full observation of the network, the proposed FOR-based constraint management method is able to be implemented under limited measurements. Due to the one-to-one correspondence between FOR boundaries and the network constraints, we simply need to include the FOR constraints of the components equipped with real-time measurements into the constraints of the optimization model. This ensures that the FOR-based method is scalable, adapting to various measurement conditions, which is promising in the transition to a highly or fully observable distribution networks in the future. Additionally, unlike sensitivity-based OPF methods, which require continuous updates of sensitivity coefficients, the FOR-based constraints remain fixed as long as the network's topology and parameters do not change.

3) The method can rapidly generate SOP set points, with the cost of time being solely dependent on the number of SOP terminals and measurement units, rather than the scale of the distribution network.

The rest of this paper is organized as follows. Section II begins with an introduction to the FOR of a distribution network. Subsequently, Section III elaborates on the development of the FOR-based control method, which is then transformed into a quadratic programming formulation in Section IV. Section V provides three-node distribution network and IEEE 33-node distribution network case studies to validate the proposed methodology and to compare it with local control and conventional OPF-based control. Section VI concludes this paper with a discussion.

## II. Preliminaries

### A. Definition of feasible operation region

A feasible operation region (FOR) is defined as the collection of operating states of a distribution network where the network constraints are not violated [19]. Fig. 1 provides a schematic representation of the FOR. Enclosed within the FOR boundaries are all feasible operating states; conversely, any operating states beyond these boundaries are infeasible. When characterizing operating states as nodal power injections in the network, the boundaries of FOR indicate the maximum limits of power injections that a distribution network can accommodate, offering insights into the network's capability of integrating generation and demand.

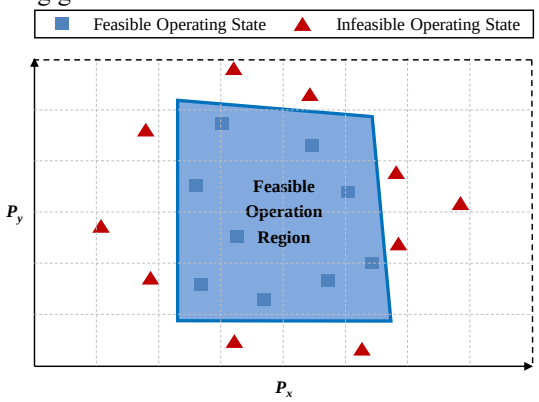


Fig. 1. Schematic representation of the feasible operation region of a distribution network. (The figure provides an example of a two-dimensional FOR in the $P_x$–$P_y$ power injection space, while in practice, a FOR is typically high-dimensional, encompassing the entire **P**–**Q** power injection space.)

It is noteworthy that the FOR is solely associated with the network topology and component parameters. Consequently, the FOR can distinctly characterize the capability of a given distribution network.

### B. Boundaries of a feasible operation region

The FOR of a distribution network is encompassed by multiple high-dimensional surfaces that are determined by thermal and voltage constraints [19]. These surfaces, also referred to as the boundaries of the FOR, ensure the network operates normally without breaching its constraints. Considering different network constraints, the FOR boundaries can be subdivided into thermal boundaries and voltage boundaries. In this study, we employ the quadratic expressions from [19] for approximating the thermal boundaries and utilize the linear/hyperplane expressions in [18] for the upper and lower voltage boundaries of the FOR.

#### 1) Thermal boundaries

The quadratic thermal boundaries are derived from the relationship between line currents and line flows [19] as follows:

$$\left(P_{ij}\right)^2+\left(Q_{ij}\right)^2=\left(V_j I_{ij}^M\right)^2,\forall ij\in B \tag{1}$$

where $B$ is the set of lines of a distribution network. $F_{iji}$, $P_{ij}$, and $Q_{ij}$ denote the current, active power flow and reactive power flow for the power line $it$. $V_j$ is the voltage magnitude for node $j$. $I_{ij}^M$ is the upper limit of the current on the power line $ij$.

As assumed in [18], [19], the power losses at the downstream nodes of node $j$ can be ignored since the power losses is small compared to the power injections, and the node voltage $V_j$ can be approximated by the voltage magnitude at the slack bus $V_0$ since the allowable variation of node voltages is small (normally within ± 3% or ± 5%). The quadratic thermal boundaries of the FOR can be then expressed as follows:

$$\left(\sum_{k=1}^{n}\alpha_k^{I_{ij}}P_k\right)^2+\left(\sum_{k=1}^{n}\beta_k^{I_{ij}}Q_k\right)^2=\left(V_0 I_{ij}^M\right)^2,\forall ij\in B \tag{2}$$

where $n$ is the number of nodes (excluding the slack bus) in the distribution network. $P_k$ and $Q_k$ are the active and reactive

power injections at node $k$ of the distribution network. Their coefficients $\alpha_k^{I_{ij}} = \beta_k^{I_{ij}} = 1$ if node $k$ is the downstream node of node $j$ (or node $k$= node $j$); otherwise $\alpha_k^{I_{ij}} = \beta_k^{I_{ij}} = 0$.

*2) Voltage boundaries*

The linear upper and lower voltage boundaries are expressed in (3) and (4) [18], respectively:

$$\sum_{k=1}^{n}\left(\alpha_k^{V_{i,M}} P_k + \beta_k^{V_{i,M}} Q_k\right) = 1, \forall i \in N \tag{3}$$

$$\sum_{k=1}^{n}\left(\alpha_k^{V_{i,m}} P_k + \beta_k^{V_{i,m}} Q_k\right) = 1, \forall i \in N \tag{4}$$

where $N$ is the set of nodes of the distribution network. $\alpha_k^{V_{i,M}} = \frac{r_k^i}{V_0\left(V_i^M - V_0\right)}$ and $\beta_k^{V_{i,M}} = \frac{x_k^i}{V_0\left(V_i^M - V_0\right)}$ are the coefficients of $P_k$ and $Q_k$ for upper voltage boundaries in (3); $\alpha_k^{V_{i,m}} = \frac{r_k^i}{V_0\left(V_i^m - V_0\right)}$ and $\beta_k^{V_{i,m}} = \frac{x_k^i}{V_0\left(V_i^m - V_0\right)}$ are the coefficients of $P_k$ and $Q_k$ for lower voltage boundaries in (4). Here $v_i^M$ and $v_i^m$ are the statuary maximum and minimum voltage limits at node $i$. It should be noted that $V_0$, $v_i^M$ and $v_i^m$ denote voltage magnitudes. The resistance $r_k^i$ and the reactance $x_k^i$ are obtained according to the topology and component parameters of the network as in (5):

$$r_k^i + jx_k^i = \begin{cases} R_{0,i} + jX_{0,i}, & \text{if } k \in D_i \text{ or } k = i \\ R_{0,k} + jX_{0,k}, & \text{if } i \in D_k \\ R_{0,s} + jX_{0,s}, & \text{if } k \notin D_i \text{ and } i \notin D_k \end{cases} \tag{5}$$

where $D_x$ ($x$=$i$ or $k$ in (5)) denotes the set of the downstream nodes of $x$. $R_{0,x} + X_{0,x}$ ($x$=$i$, $k$ or $s$ in (5)) is the total impedance of the lines from the slack node to node $x$. If node $i$ and node $k$ are on the same branch with node $k$ downstream of node $i$, then $x$=$i$. Conversely, if node $i$ is downstream of node $k$, then $x$=$k$. However, if node $i$ and node $k$ are positioned on different branches, then $x$ represents the first junction node encountered on the paths upstream from both nodes $i$ and $k$.

### C. Expressions of FOR

By integrating the thermal boundaries as given in (2) with the voltage boundaries presented in (3)-(4), we can express the FOR of a distribution network within the power injection space as follows:

$$FOR := \left\{ \left(\vec{P}, \vec{Q}\right)^T \middle| \begin{array}{l} \left(\sum_{k=1}^{n} \alpha_k^{I_{ij}} P_k\right)^2 + \left(\sum_{k=1}^{n} \beta_k^{I_{ij}} Q_k\right)^2 \le \left(V_0 I_{ij}^M\right)^2, \forall ij \in B \\ \sum_{k=1}^{n}\left(\alpha_k^{V_{i,M}} P_k + \beta_k^{V_{i,M}} Q_k\right) \le 1, \forall i \in N \\ \sum_{k=1}^{n}\left(\alpha_k^{V_{i,m}} P_k + \beta_k^{V_{i,m}} Q_k\right) \le 1, \forall i \in N \end{array} \right\} \tag{6}$$

## III. Mathematic formulation of FOR-based constraint management using SOPs

In this section, an optimization model for constraint management of a distribution network with SOPs is established. Compared to the conventional OPF-based model, constraints represented by FOR boundaries, instead of power flow equations and network constraints, are considered in the model. Due to one-to-one correspondence between FOR boundaries and thermal/voltage constraints, the formulated optimization model can adapt to various measurement conditions. Before introducing the developed model, the requirements of constraint management using SOPs are presented first.

### A. Requirements of constraint management using SOPs

The required infrastructure for constraint management of the distribution network with SOPs include real-time measurement and communication equipment for line flows and node voltages, and SOP controllers. It should be mentioned that in distribution networks, the power flows through each secondary substation (represented as the nodes in the distribution network) are generally not available in real-time [7].

Given the significant expenses associated with measurement and communication units, the available measurements under current conditions are limited. These measurements are predominantly situated at the HV/MV substation, such as the MV bus and feeder outlets. Furthermore, key line segments are also furnished with real-time line flow measurement and communication equipment to guarantee the uninterrupted operation of the distribution network.

Within the context of constraint management using SOPs, the limited real-time measurement data is forwarded by communication equipment to the SOP controllers. Utilizing these measurements, reference values (i.e., the change to the SOP set point) are determined by the SOP control algorithm (e.g., an optimization algorithm) within the SOP controllers and are then sent as a control signal to SOP converters. In response, the SOP converters make adjustments to the power set points, leading to improved performance of the distribution network.

For effective constraint management using SOPs, three critical requirements must be considered:

1) SOP control should be effective with real-time (yet limited) measurements of line currents/line flows and node voltages.

2) The control algorithm is designed for managing constraints within the distribution network. Upon detecting violations, such as thermal overloading in power lines or overvoltage/undervoltage issues at busbars via network state measurements, the algorithm should efficiently address and rectify these issues using SOPs.

3) The SOP control should adapt to real-time measurement. Specifically, the cumulative time cost, including the communication delay, the generation of SOP set points, and the hardware control of the SOP, should not exceed a measurement interval. With the advancements in communication technologies, such as the adoption of micro phaser measurement units, and the capability of SOPs to adjust their power output within milliseconds, the primary emphasis should be on developing an efficient model and algorithm for generating SOP set points rapidly.

To meet the above three requirements, an effective optimization model is established in the following subsections of this section, while an algorithm to expedite the solution of the model is developed in Section IV.

### B. Constraints

#### 1) SOP constraints

In a general case, $m$ ($m \geq 2$) feeders of the distribution network can be connected by an SOP with $m$ converters, which share the same DC bus. While active power can be transferred among the interconnected feeders, the reactive power can be either provided or absorbed at the various SOP terminals independently.

Assuming the positive direction of the active power of each SOP terminal is from the SOP terminal towards the connected node of the distribution network, the active powers controlled by SOP should follow the constraint as below:

$$\sum_{k \in \Omega_{SOP}} \left( P_{k,t}^{SOP} + \Delta P_{k,t+\Delta t}^{SOP} \right) = 0 \tag{7}$$

where $P_{k,t}^{SOP}$ is the active power output from the SOP at node $k$ at time $t$. $\Omega_{SOP}$ denotes the set of nodes connected by the SOP. $\Delta P_{k,t+\Delta t}^{SOP}$ is the adjustment in the active power set point of the SOP after a total elapsed time $\Delta t$ since time $t$. The shorter the time cost, the more prompt the SOP control will be. It should be noted that with the use of the modular multi-level converter technology, the operating loss of a converter is relatively low, approximately 1% per converter [25]. Therefore, for simplicity, the SOP losses are neglected.

Though the reactive power set points for different SOP terminals are independent, they, together with the active power set points, are constrained by the converter capacity:

$$\left( P_{k,t}^{SOP} + \Delta P_{k,t+\Delta t}^{SOP} \right)^2 + \left( Q_{k,t}^{SOP} + \Delta Q_{k,t+\Delta t}^{SOP} \right)^2 \leq S^{SOP}, \forall k \in \Omega_{SOP} \tag{8}$$

where $Q_{k,t}^{SOP}$ is the reactive power output from the SOP at node $k$ at time $t$. $\Delta Q_{k,t+\Delta t}^{SOP}$ is the adjustment in the reactive power set point of the SOP after a total elapsed time $\Delta t$ since time $t$. $S^{SOP}$ is the capacity of the converters.

#### 2) FOR constraints

From the previous study [18], [19], each FOR boundary is determined by one thermal/voltage constraint of the distribution network. The one-to-one correspondence between FOR boundaries and thermal/voltage constraints allows the use of FOR to establish the operational constraints under incomplete measurements of line flows/node voltages. For instance, when concerned with the line flow on a specific line segment, it is sufficient to incorporate the constraint of the thermal boundary, which is determined by the thermal constraint of the line flow, into the constraints of the optimization model. This feature makes the constraints of FOR boundaries more advantageous than the conventional OPF constraints which necessitate global measurements or predictions of all the power generation and load.

However, prior studies depict FOR boundaries as equations of nodal power injections, which are not directly applicable since the measurements taken are line flows and node voltages. This subsection transforms the FOR boundaries into a format based on line flows and node voltages.

*a) Thermal constraints*

The thermal boundaries of the FOR expressed in (2) provide the impact coefficients regarding each nodal power injection (i.e., $\alpha_k^{I_{ij}} = \beta_k^{I_{ij}}$) on the line flows. Considering the impact of power regulation from SOPs, the thermal boundary of any line segment $ij$ can be expressed as:

$$\begin{aligned} &\left( P_{ij,t} - \sum_{k \in \Omega_{SOP}} \alpha_k^{I_{ij}} \Delta P_{k,t+\Delta t}^{SOP} \right)^2 + \\ &\left( Q_{ij,t} - \sum_{k \in \Omega_{SOP}} \beta_k^{I_{ij}} \Delta Q_{k,t+\Delta t}^{SOP} \right)^2 = \left( V_0 I_{ij}^M \right)^2 \end{aligned} \tag{9}$$

which directly employs the measured active power flow $P_{ij,t}$ and reactive power flow $Q_{ij,t}$ on line $ij$, subtracting the downstream power injection from SOPs to indicate the line flows. It is noteworthy that in (9) node $i$ is the sending node of line $ij$ which is closer to the HV/MV substation than the receiving node $j$. In this regard, negative signs are added in the brackets at left side of the equation to express the impact of SOP power injections on the line flows. The power losses of the SOP power adjustments through the network are very small compared to $P_{ij,t}$ and $Q_{ij,t}$, which are ignored in (9). Additionally, we can define a threshold for the line capacity $I_{ij}^M$ in the FOR constraints afterwards to avoid its impact on the performance of SOP control.

Assuming $\Omega_B$ as the lines equipped with measurement units, the constraints of thermal boundaries of FOR regarding these lines then can be expressed as:

$$\begin{aligned} &\left( P_{ij,t} - \sum_{k \in \Omega_{SOP}} \alpha_k^{I_{ij}} \Delta P_{k,t+\Delta t}^{SOP} \right)^2 + \\ &\left( Q_{ij,t} - \sum_{k \in \Omega_{SOP}} \beta_k^{I_{ij}} \Delta Q_{k,t+\Delta t}^{SOP} \right)^2 \leq \left( V_0 I_{ij}^M \right)^2, \quad \forall ij \in \Omega_B \end{aligned} \tag{10}$$

*b) Voltage constraints*

Based on the voltage boundaries of FOR in (3)-(5), we can have the constraints for each node voltage as follows:

$$V_i^m \leq V_i = V_0 + \frac{1}{V_0} \sum_{k=1}^{n} \left( r_k^i P_k + x_k^i Q_k \right) \leq V_i^M, \forall i \in \Omega_N \tag{11}$$

where $\Omega_N$ are the nodes equipped with measurement units. The change of nodal power injections $P_k$ and $Q_k$ ($k \in \Omega_{SOP}$) due to the adjustment of SOP power injections will result in the change of $V_i$ at time $t+\Delta t$ as below:

$$\Delta V_{i,t+\Delta t} = \frac{1}{V_0} \sum_{k \in \Omega_{SOP}} \left( r_k^i \Delta P_{k,t+\Delta t}^{SOP} + x_k^i \Delta Q_{k,t+\Delta t}^{SOP} \right) \tag{12}$$

Considering $\Delta t$ is short, $V_{i,t+\Delta t}$ (i.e., $V_i$ at time $t+\Delta t$ under the SOP control) can be:

$$V_{i,t+\Delta t} = V_{i,t} + \Delta V_{i,t+\Delta t} \tag{13}$$

$V_{i,t+\Delta t}$ should satisfy the voltage constraints as:

$$V_i^m \le V_{i,t+\Delta t} \le V_i^M, \forall i \in \Omega_N \tag{14}$$

Through (12)-(14), we can obtain:

$$\begin{aligned} V_i^m \le V_{i,t} + \frac{1}{V_0} \sum_{k\in\Omega_{SOP}} \left( r_k^i \Delta P_{k,t+\Delta t}^{SOP} + x_k^i \Delta Q_{k,t+\Delta t}^{SOP} \right) \\ \le V_i^M, \forall i \in \Omega_N \end{aligned} \tag{15}$$

From the foregoing deduction, the FOR constraints associated with nodal power injections can be transformed into new expressions based on measurements of line flows and node voltages and the adjustments of SOP power set points as shown in (10) and (15). In general, the coefficients within the analytical expressions of the FOR boundaries reflect the impact of each nodal power injection on line currents and node voltages. These coefficients are used to account for the impact of SOP power adjustments in the thermal and voltage constraints.

### C. Objective functions

For optimal constraint management of the distribution network, three objectives, including the feeder load balancing, voltage profile improvement, and power losses reduction are used for real-time control of SOP. These three objectives have been widely used in existing studies on OPF-based SOP control [1], [3], [8]. To compare the proposed FOR-based method with the conventional OPF method provided in these studies, the same form of objective functions is used. It should be noted that the objective functions are transformed from those in the existing studies into the form associated with the active/reactive power adjustments of SOPs.

*1) Feeder load balancing*

The goal for feeder load balancing is to balance the line flows on different lines of the distribution network. With the measurement of the line flows and the power adjustments of SOPs, the feeder load balancing (FLB) index can be expressed in the form of apparent power flow as follows:

$$FLB = \sum_{ij\in\Omega_B} \frac{\left( P_{ij,t} - \sum_{k\in\Omega_{SOP}} \alpha_k^{I_{ij}} \Delta P_{k,t+\Delta t}^{SOP} \right)^2 + \left( Q_{ij,t} - \sum_{k\in\Omega_{SOP}} \beta_k^{I_{ij}} \Delta Q_{k,t+\Delta t}^{SOP} \right)^2}{S_{ij,rate}^2} \tag{16}$$

where $S_{ij,rate}$ is the rated capacity of the line $ij$. The numerator within the summation symbol represents the approximate square of the power flow on the observable lines, accounting for the impact of SOP power injections.

Since SOPs are normally connected between unbalanced feeders, the objective function leads to an optimal power control of SOPs to achieve balancing of feeder utilization [1].

*2) Voltage profile improvement*

Voltage profile index (VPI) is commonly used to measure the voltage improvement of a distribution network with SOPs [1]. The index reflects the degree of dispersion of all concerned node voltages (that are monitored by measurement units) from the nominal values, which is described as:

$$VPI = \sum_{i\in\Omega_N} \left( V_{i,t+\Delta t} - V_{i,ref} \right)^2 \tag{17}$$

$V_{i,ref}$ is the nominal voltage magnitude at bus $i$, which is set as 1.0 p.u. in this paper. $V_{i,t+\Delta t}$ is expressed as in (12) and (13). By minimizing the voltage deviation from the nominal value, the equipment of the customers connected to distribution networks can operate more efficiently, as their rated operating voltages are typically designed according to the nominal voltage of the network. Additionally, considering future scenarios where DG integration may cause voltage rise, and the electrification of transport and heating may lead to voltage drops, using the midpoint voltage is an effective strategy [8].

*3) Power losses reduction*

Power losses index (PLI), as shown in (18), is used as an objective function in the optimization model to reduce the power losses of the distribution network.

$$PLI = \sum_{ij\in\Omega_B} R_{ij} \frac{\left( P_{ij,t} - \underbrace{\Delta P_{k,t+\Delta t}^{SOP}}_{\text{if } k\in\Omega_{SOP}\cap D_j} \right)^2 + \left( Q_{ij,t} - \underbrace{\Delta Q_{k,t+\Delta t}^{SOP}}_{\text{if } k\in\Omega_{SOP}\cap D_j} \right)^2}{V_0^2} \tag{18}$$

$R_{ij}$ is the resistance of line $ij$. $V_0$ is used for approximating the node voltages at node $i$ for calculating the losses of line $ij$.

### D. Optimization Model

The decision variables of the optimization problem are $\Delta P_{k,t+\Delta t}^{SOP}$ and $\Delta Q_{k,t+\Delta t}^{SOP}$ ( $\forall k \in \Omega_{SOP}$ ). The full optimization model for the real-time control of SOPs is shown below:

minimize (16) or (17) or (18)
subject to (7), (8), (10), (15)

The model solves the power adjustments of SOPs at time $t$ with a time delay $\Delta t$. The model demonstrates scalability as the corresponding thermal/voltage constraint can be appended for each concerned line/node with a measurement. Consequently, the optimization model can be implemented regardless of the number of measurement units installed in the distribution network, especially applicable to current situation with incomplete measurement.

### E. Comparison with existing OPF models

To highlight the benefits of the proposed FOR-based model, two commonly used OPF models for SOP control are compared in detail as follows.

*1) Conventional OPF model*

The conventional OPF model for SOP control in distribution networks incorporates power flow equations and network constraints within the optimization formulation, which aims to optimize the power control of SOPs such that the index of voltage profile, line flow profile, or the power losses in the objective function is the minimum [1], [3]. Let **x** be the vector of nodal power injections and let **y** be the vector of power injections from SOP terminals. The conventional OPF for SOP control can be formulated in the compact form as below:

$$\min f(\mathbf{V},\mathbf{I})$$
$$s.t.\begin{cases} g_1(\mathbf{P}_{\text{Line}},\mathbf{Q}_{\text{Line}},\mathbf{I}) = \mathbf{x}+\mathbf{y} \\ g_2(\mathbf{V},\mathbf{I},\mathbf{P}_{\text{Line}},\mathbf{Q}_{\text{Line}}) = 0 \\ g_3(\mathbf{y}) = 0 \\ h(\mathbf{y}) \le 0 \\ \mathbf{V_m} \le \mathbf{V} \le \mathbf{V_M} \\ |\mathbf{I}| \le \mathbf{I_M} \end{cases} \tag{19}$$

where the equality equations $g_1$ and $g_2$ represent the power flow equations based on disflow branch model [1], [3], whereas the equality $g_3$ describes SOP active power constraints. The inequality equations include the SOP capacity constraints $h$, voltage constraints and line currents constraints. Further details for these constraints can also refer to [1], [3], [6].

In (19), the state variables include the voltage magnitudes $\mathbf{V}$, line flows $\mathbf{P}_{\text{Line}}$ and $\mathbf{Q}_{\text{Line}}$, and line currents $\mathbf{I}$. These state variables are determined by the global information of nodal power injections (i.e., known variables $\mathbf{x}$) and the power output of SOPs (i.e., decision variables $\mathbf{y}$). Therefore, the conventional OPF method cannot be used under incomplete measurement conditions. In practice, the measurements of nodal power load and generation are normally not accessible online [7].

In contrast, the proposed FOR-based model is free of power flow equations. The new formula of FOR constraints (see (10) and (15)) within the proposed FOR-based model only requires the observable line flows and node voltages, which allows for the use of these real-time measurements. Moreover, the one-to-one correspondence between FOR constraints and the network constraints makes the method scalable and adaptable to various measurement conditions.

*2) Sensitivity-based OPF model*

Rather than using power flow equations, the sensitivity-based OPF describes the line currents and node voltages in response to SOP power adjustments based on sensitivity analysis. The key to the sensitivity analysis is to obtain the voltage-to-power and line flow-to-power sensitivity coefficients, which can be commonly obtained by two approaches: the Jacobian matrix-based approach [8] and the perturb-and-observe power flow-based approach [9], [10].

The first approach is to extract the voltage sensitivity coefficients from the Jacobian matrix under the Newton Raphson power flow calculation [8]. In contrast, the latter approach, though not yet used in SOP control, can calculate the sensitivity coefficients by introducing a unit power change from the SOPs and performing a snapshot power flow, maintaining the same load and generation levels [10]. The resulting line flow or node voltage from this unit power change is then used to estimate the sensitivity coefficients.

Both approaches require the full observation of the load and generation conditions, as they rely on Jacobian matrix calculations or power flow analysis. In addition, the sensitivity coefficients need to be continuously updated since these coefficients change as load and generation conditions vary [8-10].

The formulation of the sensitivity-based OPF is similar with that of the proposed FOR-based model, both using coefficients to evaluate the impact of nodal power changes on line currents and node voltages. However, the coefficients used in the FOR-based model are constant as long as the topology and parameters of the network do not change. Furthermore, the proposed FOR-based model can be applied under limited observability of the network.

*3) Summary*

Compared to the conventional OPF and sensitivity-based OPF models, which rely on global measurements of power load and generation, the FOR-based method can adapt to various measurement conditions. Notably, the coefficients for the FOR-based model remain constant given a fixed network topology and parameters, making it more convenient to use than the sensitivity-based OPF. It is also worth mentioning that, since the conventional OPF method provides the optimal control strategy for SOPs (if the global measurements are assumed available), it will serve as a reference for comparison with the proposed FOR-based method in the case studies in Section V.

## IV. Quadratic programming conversion

The proposed FOR-based model in Section III is a nonlinear optimization model due to the quadratic objective functions in (16)-(18) and quadratic constraints in (8) and (10). This section further converts the nonlinear optimization model to a quadratic programming model, which can be effective in real-time constraint management of the distribution network with SOPs.

In this section, we begin by introducing auxiliary state variables for the SOP set points, line flows, and node voltages. Subsequently, we linearize the quadratic constraints within the model to facilitate its transition to a quadratic programming framework. As a result, the optimization model is formulated in matrix form, where the matrices and coefficient vectors irrelevant to the measurements are segregated. Because these segregated matrices and coefficient vectors can be prepared offline, the computation time of the optimization problem can be further reduced.

### A. Introduction of state variables

Before the conversion, we first introduce auxiliary state variables of SOP set points, line flows and node voltages to simplify the expressions of the model in Section III. D.

Regarding the SOP set points, we define the state variables of SOP set points at time $t+\Delta t$ as below:

$$P_{k,t+\Delta t}^{SOP} = P_{k,t}^{SOP} + \Delta P_{k,t+\Delta t}^{SOP} \tag{20}$$

$$Q_{k,t+\Delta t}^{SOP} = Q_{k,t}^{SOP} + \Delta Q_{k,t+\Delta t}^{SOP} \tag{21}$$

The state variables of line flows are introduced in (22)-(23). The variables express the approximate line flows on each measured line at time $t+\Delta t$.

$$P_{ij,t+\Delta t} = P_{ij,t} - \sum_{k\in\Omega_{SOP}} \alpha_k^{I_{ij}} \Delta P_{k,t+\Delta t}^{SOP} \tag{22}$$

$$Q_{ij,t+\Delta t} = Q_{ij,t} - \sum_{k\in\Omega_{SOP}} \beta_k^{I_{ij}} \Delta Q_{k,t+\Delta t}^{SOP} \tag{23}$$

With respect to node voltages, we have the voltage variable $V_{i,t+\Delta t}$ by substituting (12) in (13) as below:

$$V_{i,t+\Delta t} = V_{i,t} + \frac{1}{V_0}\sum_{k\in\Omega_{SOP}}\left(r_k^i \Delta P_{k,t+\Delta t}^{SOP} + x_k^i \Delta Q_{k,t+\Delta t}^{SOP}\right) \quad (24)$$

With the introduction of state variables, both the objective functions and the constraints in the model of Section III. D can be simplified, facilitating their conversion into the standard matrix form of the quadratic programming model.

### *B. Linearization of the quadratic constraints*

A polygonal inner-approximation method is employed to linearize the capacity constraints for SOP in (8) and the thermal constraints in (10) since they are both in circular form. In this paper, we use a regular polygon with 12 edges for the linearization. After substituting (20)-(21) into (8) and (22)-(23) into (10), (8) and (10) can be linearized via polygonal inner-approximation as follows:

$$\alpha_c P_{k,t+\Delta t}^{SOP} + \beta_c Q_{k,t+\Delta t}^{SOP} + \delta_c S^{SOP} \le 0,\ \forall c \in \{1,2,...,12\} \quad (25)$$

$$\alpha_c P_{ij,t+\Delta t} + \beta_c Q_{ij,t+\Delta t} + \delta_c \left(V_0 I_{ij}^M\right) \le 0,\ \forall c \in \{1,2,...,12\} \quad (26)$$

where the values of the coefficients can refer to [21] and are no longer repeated in this paper.

Since the linearization through the polygonal inner-approximation method is conservative, the operating state of the distribution network that satisfies (25) and (26) will not violate the capacity constraints for SOP in (8) and the thermal constraints in (10).

### *C. Formulation of the quadratic programming model*

Through the above conversion, the three objective functions (16)-(18) of the optimization model can be simplified as:

$$FLB = \sum_{ij\in\Omega_B} \frac{\left(P_{ij,t+\Delta t}\right)^2 + \left(Q_{ij,t+\Delta t}\right)^2}{S_{ij,rate}^2} \quad (27)$$

$$VPI = \sum_{i\in\Omega_N} \left(V_{i,t+\Delta t} - V_{i,ref}\right)^2 \quad (28)$$

$$PLI = \sum_{ij\in\Omega_B} R_{ij} \frac{\left(P_{ij,t+\Delta t}\right)^2 + \left(Q_{ij,t+\Delta t}\right)^2}{V_0^2} \quad (29)$$

The optimization model is then formulated as follows:

$$\min (26) or (27) or (28)$$

$$s.t.\begin{cases} \sum_{k\in\Omega_{SOP}} P_{k,t+\Delta t}^{SOP} = 0 \\ \alpha_c P_{k,t+\Delta t}^{SOP} + \beta_c Q_{k,t+\Delta t}^{SOP} + \delta_c S^{SOP} \le 0,\ \forall c \in \{1,2,...,12\} \\ \alpha_c P_{ij,t+\Delta t} + \beta_c Q_{ij,t+\Delta t} + \delta_c \left(V_0 I_{ij}^M\right) \le 0,\ \forall c \in \{1,2,...,12\} \\ V_i^m \le V_{i,t+\Delta t} \le V_i^M, \forall i \in \Omega_N \\ P_{k,t+\Delta t}^{SOP} = P_{k,t}^{SOP} + \Delta P_{k,t+\Delta t}^{SOP},\ \forall k \in \Omega_{SOP} \\ Q_{k,t+\Delta t}^{SOP} = Q_{k,t}^{SOP} + \Delta Q_{k,t+\Delta t}^{SOP},\ \forall k \in \Omega_{SOP} \\ P_{ij,t+\Delta t} = P_{ij,t} - \underbrace{\Delta P_{k,t+\Delta t}^{SOP}}_{\text{if } k\in\Omega_{SOP}\cap D_j},\ \forall ij \in \Omega_B \\ Q_{ij,t+\Delta t} = Q_{ij,t} - \underbrace{\Delta Q_{k,t+\Delta t}^{SOP}}_{\text{if } k\in\Omega_{SOP}\cap D_j},\ \forall ij \in \Omega_B \\ V_{i,t+\Delta t} = V_{i,t} + \frac{1}{V_0}\sum_{k\in\Omega_{SOP}}\left(r_k^i \Delta P_{k,t+\Delta t}^{SOP} + x_k^i \Delta Q_{k,t+\Delta t}^{SOP}\right), \forall i \in \Omega_N \end{cases} \quad (30)$$

The variables of the model in (30) include the decision variables $\Delta P_{k,t+\Delta t}^{SOP}$ and $\Delta Q_{k,t+\Delta t}^{SOP}$ and the state variables $P_{k,t+\Delta t}^{SOP}$, $Q_{k,t+\Delta t}^{SOP}$, $P_{ij,t+\Delta t}$, $Q_{ij,t+\Delta t}$, and $V_{i,t+\Delta t}$. Defining the vector of the decision variables as $X_1$ and the vector of the state variables as $X_2$, the compact form of the model (30) is shown below:

$$\min \frac{1}{2}\boldsymbol{X}_2^{\boldsymbol{T}}\boldsymbol{H}\boldsymbol{X}_2 + \boldsymbol{f}^{\boldsymbol{T}}\boldsymbol{X}_2 + \boldsymbol{c}$$

$$\text{s.t.}\begin{cases} \boldsymbol{A_{eq}}\boldsymbol{X}_2 = \boldsymbol{b_{eq}} \\ \boldsymbol{A}\boldsymbol{X}_2 \le \boldsymbol{b} \\ \boldsymbol{l_b} \le \boldsymbol{X}_2 \le \boldsymbol{u_b} \\ \boldsymbol{X}_2 = \boldsymbol{D}\boldsymbol{X}_1 + \boldsymbol{e_t} \end{cases} \quad (31)$$

(31) includes the linear equality from the first constraint of (30), the linear inequality from the second and third constraints of (30), the lower and upper bounds from the fourth constraint of (30) and the linear relationship between $\boldsymbol{X_1}$ and $\boldsymbol{X_2}$, which is shown in the last five constraints of (30). Here $\boldsymbol{e_t}$ is the vector of state variables (i.e., $\boldsymbol{e_t}$ = ( $P_{k,t+\Delta t}^{SOP}$, $Q_{k,t+\Delta t}^{SOP}$, $P_{ij,t+\Delta t}$, $Q_{ij,t+\Delta t}$, $V_{i,t+\Delta t}$ )$^T$). By substituting $\boldsymbol{X_2}=\boldsymbol{D}\boldsymbol{X_1}+\boldsymbol{e_t}$ in the model, we can finally obtain the quadratic programming model as in (32).

$$\min \frac{1}{2}\boldsymbol{X}_1^{\boldsymbol{T}}\tilde{\boldsymbol{H}}\boldsymbol{X}_1 + \tilde{\boldsymbol{f}}_{\boldsymbol{t}}^{\boldsymbol{T}}\boldsymbol{X}_1 + \tilde{\boldsymbol{c}}_{\boldsymbol{t}}$$

$$\text{s.t.}\begin{cases} \left(\boldsymbol{A_{eq}}\boldsymbol{D}\right)\boldsymbol{X}_1 = \boldsymbol{b_{eq}} - \boldsymbol{A_{eq}}\boldsymbol{e_t} \\ \left(\boldsymbol{A}\boldsymbol{D}\right)\boldsymbol{X}_1 \le \boldsymbol{b} - \boldsymbol{A}\boldsymbol{e_t} \\ \boldsymbol{D}^{-1}\left(\boldsymbol{l_b} - \boldsymbol{e_t}\right) \le \boldsymbol{X}_1 \le \boldsymbol{D}^{-1}\left(\boldsymbol{u_b} - \boldsymbol{e_t}\right) \end{cases} \quad (32)$$

$\tilde{\boldsymbol{H}}$ and $\tilde{\boldsymbol{f}}_{\boldsymbol{t}}$ can be obtained as follows:

$$\tilde{\boldsymbol{H}} = \boldsymbol{D}^{\boldsymbol{T}}\boldsymbol{H}\boldsymbol{D} \quad (33)$$

$$\tilde{\boldsymbol{f}}_{\boldsymbol{t}} = \boldsymbol{D}^{\boldsymbol{T}}\boldsymbol{H}^{\boldsymbol{T}}\boldsymbol{e_t} + \boldsymbol{D}^{\boldsymbol{T}}\boldsymbol{f} \quad (34)$$

In (32), $\tilde{\boldsymbol{f}}_{\boldsymbol{t}}$, $\tilde{\boldsymbol{c}}_{\boldsymbol{t}}$ and $\boldsymbol{e_t}$ are associated with the measurements at time *t*. $\tilde{\boldsymbol{c}}_{\boldsymbol{t}}$ is a constant and can be removed from the objective function. $\tilde{\boldsymbol{f}}_{\boldsymbol{t}}$ and $\boldsymbol{e_t}$ should be updated during each measurement interval as the input of the optimal control. In contrast, $\tilde{\boldsymbol{H}}$, $\boldsymbol{A_{eq}}$, $\boldsymbol{b_{eq}}$, $\boldsymbol{A}$, $\boldsymbol{b}$, $\boldsymbol{l_b}$, $\boldsymbol{u_b}$ and $\boldsymbol{D}$ are irrelevant to the measurements at time *t* and can be prepared offline.

Compared with (31), the number of variables and the number of constraints in (32) are largely reduced. In general, we only have 2*m* (*m* is the number of SOP terminals) variables of $\Delta P_{k,t+\Delta t}^{SOP}$ and $\Delta Q_{k,t+\Delta t}^{SOP}$, while the number of constraints are determined by the number of SOP terminals and the number of lines and nodes that are equipped with measurement units. This indicates that the proposed model is almost not affected by the scale of the distribution network. The complexity of solving the model is only determined by the number of SOP terminals and the number of the measurement units.

## V. CASE STUDIES

In this section, first we use the IEEE 33-node distribution network to validate the proposed FOR-based real-time SOP control for the constraint management of the case network. The

performance of the proposed method under different measurement conditions are analyzed and compared to that of the local control method and the conventional OPF-based method. To verify the scalability of the proposed FOR-based constraint management method on large-scale distribution networks under differernt load and generation scenarios, the modified IEEE 123-node benchmark distribution network is further used. The computation of the case study was performed in Matlab R2019b on a PC with an Intel(R) Core(TM) i5-9300H CPU @ 2.40 GHz processor and 8 GB RAM. The Quadprog, Fmincon, and Gurobi solvers are used in Matlab to implement the proposed model, the conventional OPF model, and the simplified OPF model by cone relaxation, respectively.

### *A. IEEE 33-node distribution network*

#### *1) Assumptions*

The 12.66 kV IEEE 33-node benchmark distribution network [22] is further used to validate the effectiveness of the FOR-based constraint management method. The total active and reactive power loads of the power network are 3.715MW and 2.3MVar, respectively.

As shown in Fig. 2, we consider installation of four PV units (each rated at 1.2 MW) in the network. One 1MVA SOP is also employed at one normally open tie line to connect the ends of two feeders (i.e., node 18 and node 33). We add two nodes (node $T_1$ and node $T_2$) at the two terminals of SOP, assuming the impedance of the tie line at 0.25+j0.25 Ω.

To fully demonstrate the thermal and voltage constraint management using the SOP, we assume the thermal capacity of the transformer at 1 kA and the thermal capacity of the each line at 0.25 kA. The peak load in [22] is increased by 8%. The load profile and the PV generation profile in Fig. 3 are used in this case. Without constraint management by using the SOP, the node voltages and line currents during a day are shown in Fig. 4. Note that except line 18-$T_1$ and line 33-$T_2$, the line number of line x-y (where node x is upstream of node y) is noted as y-1 for brevity.

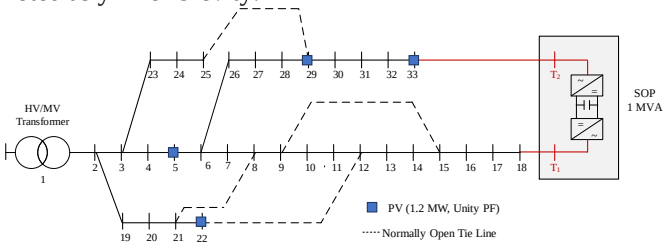


Fig. 2. Modified IEEE 33-node distribution network.

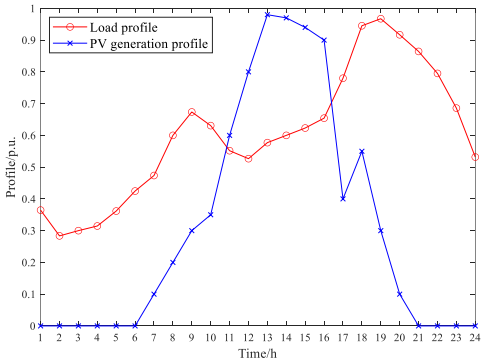


Fig. 3. Daily load profile and PV generation profile.

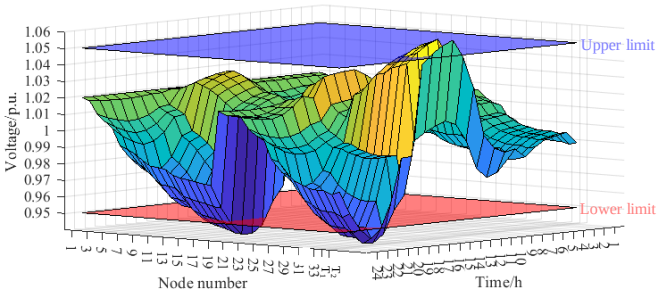


(a)

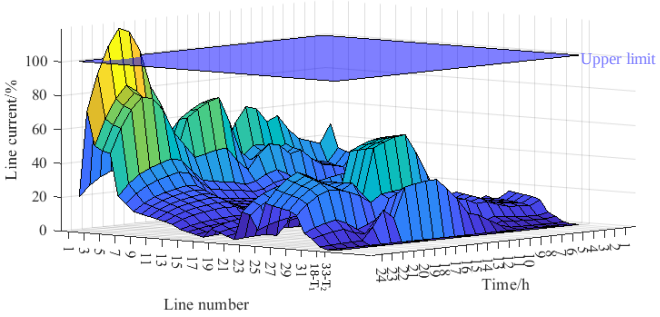


(b)

Fig. 4. Daily spatial-temporal distribution of (a) node voltages and (b) line currents of the modified IEEE 33-node distribution network without SOPs.

During 13:00-15:00, nodes on the top feeder (i.e., nodes 30-33 and node $T_2$) experience overvoltage problems. Nodes 13-18 and node $T_1$ on the bottom feeder and nodes 30-33 and node $T_2$ on the top feeder experience undervoltage problems during different hours between 19:00-22:00. During 20:00-21:00, line 2-3 experiences the overloading problem.

The performance of the FOR-based constraint management method under three different measurement conditions is compared with local control [11] and conventional OPF-based control [3] in this section. The three measurement conditions for the FOR-based method are as follows:

a) Local measurement (LM). Measurements at the SOP station are available, which include voltage measurements at node $T_1$ and node $T_2$ and line flow measurements on line 18-$T_1$ and line 33-$T_2$.

b) Moderate measurement (MM). Referring to [7], in addition to the local measurements at the SOP station, real-time measurements at the HV/MV substation and critical lines are also considered available for moderate measurement condition. The added measurements include line flow measurements at the feeder outlets of the HV/MV substation (i.e., line 2-3 and line 2-19) and the line segments (i.e., line 6-7 and line 6-26).

c) Global measurement (GM). All the lines are equipped with line flow measurements and all nodes are equipped with voltage measurements.

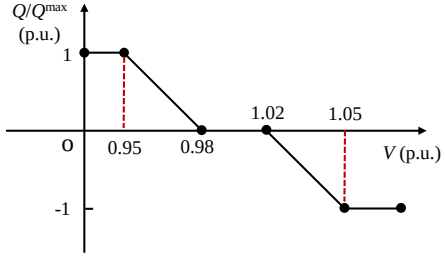


Fig. 5. Q-V curve for local control of the SOP in the modified IEEE 33-node distribution network.

The local control considered as a reference method can be achieved by using Q-V curve with the measurement of the voltages at the terminals of the SOP [11]. The parameters of the Q-V curves (which can be obtained by the method in [11]) for the two terminals of SOP in this study are selected as in Fig. 5.

Considering the SOP control objectives can be feeder load balancing, voltage profile improvement and power losses reduction (see Section III. C), we use three corresponding indices [1] in (35)-(37) respectively to evaluate the performance under different SOP control methods and measurement conditions. *B* and *N* are the set of lines and the set of nodes of the distribution network respectively.

$$LB_{index} = \sum_{t}\sum_{i\in B}\left(\frac{I_i}{I_{i\_rate}}\right)^2 \tag{35}$$

$$VP_{index} = \sum_{t}\sum_{i\in N}\left(V_{i,t} - V_{i,ref}\right)^2 \tag{36}$$

$$E_{loss} = \sum_{t}\sum_{i\in B} I_i^2 r_i \tag{37}$$

*2) Results analysis*

(a) Constraints violation

The results of the node voltages and the line currents of the distribution network under local control, conventional OPF-based control and FOR-based control are summarized in TABLE 1. The results with no SOP control are also listed for reference.

TABLE 1 Results of the voltage range and the maximum line current in the modified IEEE 33-node distribution network with SOPs during a day. (The voltages/ line currents marked in red indicate that they exceed the normal voltage range 0.95p.u.-1.05p.u./ the line capacity 100%.)

| Control method | Measurement condition | Control objective | Minimum voltage-maximum voltage | Maximum line current |
|---|---|---|---|---|
| No control | — | — | 0.94 p.u.-1.06 p.u. | 117.8% |
| Local control | LM | — | 0.98 p.u.-1.04 p.u. | 99.1% |
| FOR-based control | LM | FLB | 0.95 p.u.-1.05 p.u. | 113.3% |
| | | VPI | 0.98 p.u.-1.04 p.u. | 99.3% |
| | | PLR | 0.95 p.u.-1.05 p.u. | 113.3% |
| | MM | FLB | 0.98 p.u.-1.05 p.u. | 98.9% |
| | | VPI | 0.98 p.u.-1.04 p.u. | 99.3% |
| | | PLR | 0.98 p.u.-1.05 p.u. | 98.9% |
| | GM | FLB | 0.97 p.u.-1.05 p.u. | 98.9% |
| | | VPI | 0.98 p.u.-1.04 p.u. | 99.1% |
| | | PLR | 0.97 p.u.-1.05 p.u. | 98.9% |
| Conventional OPF-based control | GM | FLB | 0.97 p.u.-1.05 p.u. | 100.0% |
| | | VPI | 0.98 p.u.-1.04 p.u. | 100.0% |
| | | PLR | 0.97 p.u.-1.05 p.u. | 100.0% |

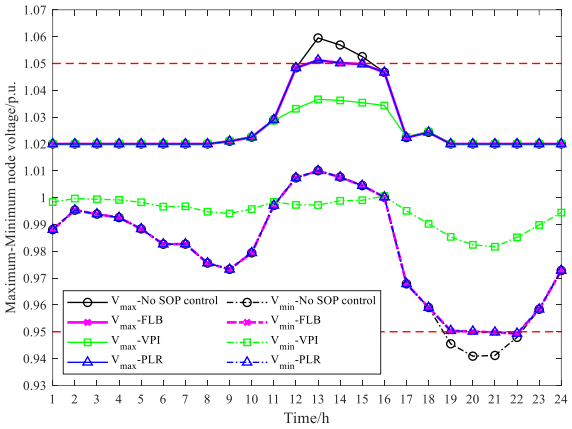


Fig. 6. Maximum and minimum voltages in the IEEE 33-node distribution network under FOR-LM control with different control objectives.

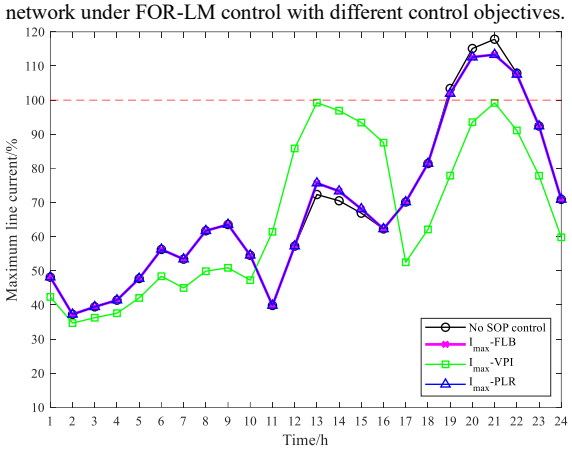


Fig. 7. Maximum line currents in the IEEE 33-node distribution network under FOR-LM control with different control objectives.

From TABLE 1, the FOR-based control method with moderate/global measurement, local control and conventional OPF-based control can solve the violation problems shown in Fig. 4, except the FOR-based control method with local measurement (termed as FOR-LM control for brevity). For clarity, the daily curves of node voltages and the line currents of the distribution network under FOR-LM control are presented in Fig. 6 and Fig. 7 respectively.

From Fig. 6 and Fig. 7, when using feeder load balancing (FLB)/ power losses reduction (PLR) as the SOP control objective, FOR-LM control can only solve the overvoltage and undervoltage problems. The overloading problems (i.e., overloading on line 2-3) can be relieved but still remains. The reason is that the line flow on line 2-3 is unobservable under FOR-LM control. In addition, the observable lines are far away from line 2-3. Therefore, the optimization of the observable line flows has little contribution to the reduction of line flow on line 2-3. In contrast, using voltage profile improvement (VPI) as the SOP control objective, FOR-LM control can solve both the thermal and voltage violation problems. This indicates that improving the voltage profile (especially at the end nodes of the feeders) might benefit the distribution of line flows across the whole network, thus solving the overloading problem in this case.

(b) Performance indices

The performance indices of different SOP control methods are obtained and shown in Fig. 8. Notably, we compare the load balancing index ($LB_{index}$) when using feeder load balancing as

the objective function in both the FOR-based constraint management model and conventional OPF-based model from [3]. Meanwhile, we compare the voltage profile index ($VP_{index}$) and energy losses ($E_{loss}$) when using voltage profile improvement and power losses reduction as SOP control objectives.

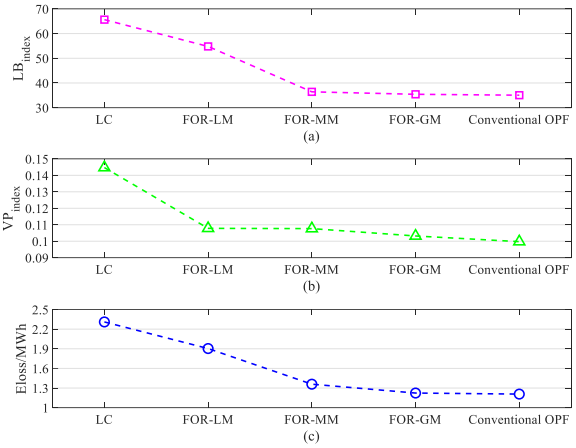


Fig. 8. Comparison of different SOP control methods in terms of: (a) feeder load balancing; (b) voltage profile improvement; (c) energy losses reduction.

In Fig. 8, the results for FOR-LM control are given for reference. Even with local measurement, the FOR-based method outperforms the local control method in all the three aspects. This is because the FOR-based method is formulated as an optimization programme which strives for the optimal solution in terms of the three control objectives, rather than merely ensuring the observable node voltages/line flows be within the network constraints. In comparison with the conventional OPF-based control, the performance of FOR-GM control is nearly the same as the conventional OPF-based method. This validates that the FOR constraints in FOR-based method can be used to replace the power flow equations and network constraints in conventional OPF-based method. Moreover, from the results in Fig. 8, the performance of the FOR-based method approaches to conventional OPF-based method with increasing measurements. It is worth noting that if the SOP control objective is voltage profile improvement, the performance of the FOR-based method can approach the optimum even with local measurement.

(c) Required computation time

The required computing time for different SOP control methods are also compared in TABLE 2. With the number of measurements increased, the network constraints to be considered by the FOR-based method rises, thus requiring more computation time for generating SOP set points. Under the "worst" case (i.e., global measurement), the computation time using the FOR-based method can be within 120 milliseconds (which is less than 1/18 of the time required by the conventional OPF-based method on average).

TABLE 2 Computing time required by different SOP control methods.

| SOP control method | Time for generating SOP set points | |
|---|---|---|
| | Average time/ms | Maximum time/ms |
| LC | 0.05 | 0.94 |
| FOR-LM | 0.80 | 5.39 |
| FOR-MM | 2.70 | 6.90 |
| FOR-GM | 64.81 | 119.15 |
| Conventional OPF | 1184.65 | 2930.20 |

In summary, the FOR-based method can adapt to any measurement conditions. It can optimize the line flow distribution and voltage profiles while ensuring the observable line currents and node voltages within their limitations. The performance of the FOR-based control method relies on both the SOP control objectives and the measurement conditions. In this study, VPI is a best choice among the control objectives. With respect to the measurement conditions, global measurement ensures the optimal performance of the whole network, which is nearly the same with the conventional OPF-based control. In contrast, moderate measurement (with only 8/70 measurement units compared to the conventional OPF-based control) can help the FOR-based method largely increases the computational efficiency, while achieving near-global optimization compared with the results with global measurement. This indicates that the developed FOR-based method, if with measurements well planned, can achieve efficient SOP control. The costs of installing measurement units can also be largely reduced.

### *B. IEEE 123-node distribution network*

To verify the scalability of the proposed FOR-based constraint management method on large-scale distribution networks, the modified IEEE 123-node distribution network is used. The structure of the network is shown in Fig. 9, where an SOP rated at 1 MVA is installed. Similar with the IEEE 33-node distribution network, the allowable voltage range for the modified IEEE 123-node network is 0.95-1.05 p.u.. The detailed network parameters can refer to [6].

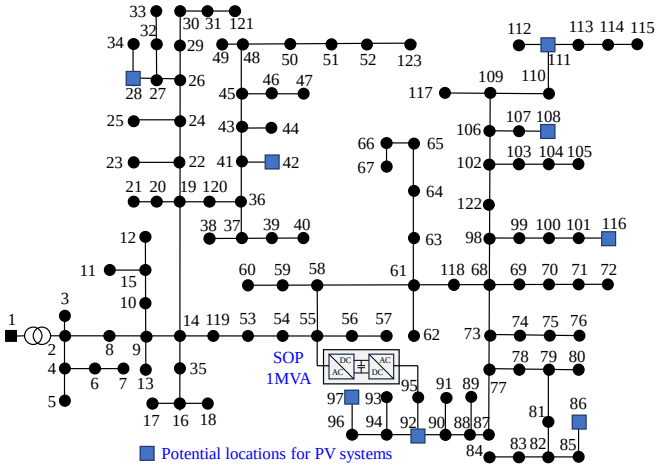


Fig. 9. Structure of the modified IEEE 123-node distribution network.

In order to fully consider the impact of high load and high generation on distribution networks, three scenarios are tested as follows:

*Scenario I:* High load scenario. The total power load within the network is 3.49 MW and 1.92 Mvar as set in [6] but without DG installation. Under this scenario, the voltage drops significantly through the long branches of the network.

*Scenario II:* Scenario with 100% DG penetration. Eight PV systems with a total capacity of 3.5 MW are installed: one PV system rated at 1 MW is installed at node 97; two PV systems, each rated at 0.5 MW, are installed at nodes 92 and 108; five PV systems rated at 0.3 MW each are located at nodes 28, 42,

86, 111, and 116. The locations and ratings of these PV systems can refer to [6].

*Scenario III:* High generation scenario. Compared to Scenario II, 60% increase in DG penetration is considered. Voltage rise in peak generation hours will occur due to increasing reverse power flow.

Given the prominence of voltage issues, the control objective for the SOP is set as improving the voltage profile, as outlined in (17). The results of the FOR-based method for SOP control are summarized and compared with the conventional OPF-based method in TABLE 3. Note that the conventional OPF-based method is used as reference, which can only be implemented with global measurement of power load and generation at different nodes of the network. In contrast, the FOR-based method can adapt to various measurement conditions. Similar to the IEEE 33-node distribution network, the local measurement condition is considered as installing real-time measurement units at the SOP terminals, while the global measurement condition assumes measurement units are equipped throughout the network. Regarding the moderate measurement condition, real-time measurement units are installed at the SOP terminals, the substation, and the locations where normally closed switches are implemented (as specified in [23]). These include line flow measurement units on power lines 1-2, 14-119, 19-120 and 61-118, and voltage measurement units at nodes 2, 14, 19, 55, 61 and 95.

From TABLE 3, without implementing the SOP, the network faces different voltage violation problems under the three testing scenarios. The proposed FOR-based method can be effective for constraint management even under incomplete measurement conditions. The voltage deviation throughout the network can be largely reduced compared to the condition without SOP implementation. In addition, the proposed method can generate SOP setpoints within a few hundred milliseconds, which can fully utilize the fast power control of SOPs to achieve real-time constraint management.

Compared to the performance of the conventional OPF-based method, the FOR-based method can achieve near-global optimal results. As the available measurement increases, the performance index will be improved. The proposed FOR-based method has two outstanding benefits as follows:

1) Since the proposed method can adapt to various measurement condition, it is promising in placing much fewer measurement units in appropriate locations to achieve the near-global optimal constraint management of the network. With less than 10 measurement units (see the local and moderate measurement conditions), the voltage index $VP_{index}$ can be largely improved already. The difference of $VP_{index}$ between the proposed method and the conventional OPF method is very small, which is less than 0.18, but the OPF method requires 244 measurement units.

2) The proposed FOR-based method is encouraging in the computational efficiency. Even equipped with global measurement as the conventional OPF requires, the proposed method only requires less than a few hundred milliseconds for generating SOP set points. Since the number of variables and constraints within the FOR-based model are solely dependent on the number of SOP terminals and measurement units, the cost of time will almost not be affected by the scale of the distribution network. This feature facilitates the proposed method to conduct real-time constraint management of the network.

In this case study, we also implement both the interior-point method and cone relaxation method [3] in solving the conventional OPF model. The results show that the interior-point method is effective in constraint management and performs very well in minimizing the voltage deviation. However, it is time consuming, taking 4-6 minutes to generate the SOP set points. In contrast, the cone relaxation method, although commonly used in distribution network analysis, fails to ensure that the network operates within its limits in Scenario I and Scenario II with high DG penetration. This issue has also been observed in several studies [24], [25]. This suggests that the optimization results for the OPF model with the cone relaxation should be carefully examined before used for network constraint management.

TABLE 3 Camparison of the performance of the FOR-based method and conventional OPF-based method for constraint management of the modified IEEE 123-node distribution network. (Algorithms selected for solving conventional OPF-based model: interior-point method (IPM); conic relaxation method (CRM) [3])

| Comparison | Whether all the constraints are satisfied or not | | | | | | Voltage index $VP_{index}/10^{-2}$ | | | | | | Average computation time for generating SOP set points/ms | | | | |
|---|---|---|---|---|---|---|---|---|---|---|---|---|---|---|---|---|---|
| SOP control method | No SOP | FOR-based method | | | Conventional OPF-based method | | No SOP | FOR-based method | | | Conventional OPF-based method | | FOR-based method | | | Conventional OPF-based method | |
| | | | | | IPM | CRM | | | | | IPM | CRM | | | | IPM | CRM |
| Measurement condition | — | LM | MM | GM | GM | GM | — | LM | MM | GM | GM | GM | LM | MM | GM | GM | GM |
| Scenario I | × Undervoltage at nodes 48-52, 58-118, 122-123 | √ | √ | √ | √ | √ | 368 | 31 | 23 | 15 | 13 | 71 | 3 | 5 | 82 | 243,000 | 674 |
| Scenario II | × Undervoltage at nodes 61-118, 122 | √ | √ | √ | √ | × Overvoltage at nodes 90, 92-94 and 96-97 | 202 | 25 | 19 | 12 | 10 | 143 | 3 | 5 | 384 | 368,000 | 965 |
| Scenario III | × Undervoltage at nodes 61-118, 122; overvoltage at nodes 93-94, 96-97 | √ | √ | √ | √ | × Overvoltage at nodes 85-97 and 107-117 | 199 | 24 | 21 | 12 | 10 | 174 | 2 | 5 | 92 | 119,000 | 1923 |

## VI. Conclusions and discussions

This paper develops a FOR-based constraint management method for distribution networks with SOPs. The conclusions are as follows:

1) The proposed FOR-based constraint management method can adapt to various measurement conditions. For effective management of a specific network constraint, the method simply requires the measurement of the specific node voltage/line flow and the addition of the corresponding FOR constraint within the optimization paradigm. By selecting different SOP control objectives, the method can be effective in optimizing the line flow distribution or node voltage profile of the observable parts of the distribution network. Whatever the control objective is used for SOPs, the observable line flows/node voltages can be managed within their limitations.

2) Using the FOR-based control method, even equipped with limited measurement units, can achieve near-global optimum results as the conventional OPF-based method. In addition, the method can rapidly generate SOP set points with the cost of time being solely dependent on the number of SOP terminals and measurement units, rather than the scale of the distribution network. Even when equipped global measurements for constraint management across the entire network, the FOR-based method can generate SOP set points within a few hundred milliseconds.

It is worthy of noting that the FOR-based constraint management method cannot ensure managing the unobservable nodes/lines of the network within their limitations. Under the circumstance where the network components with violation problems are not measured, voltage profile improvement is suggested to be used as the control objective in the FOR-based constraint management method. Currently, measurement units are typically installed at substation buses, near load centers, and on power lines that intersect branches or have a history of overloading. Considering the increasing integration of distributed generation and new electrified loads in the future, appropriate planning of measurement units in bottlenecks of distribution networks is important for the performance of the proposed FOR-based method and will be further investigated in the future.

## References


[1] X. Jiang, Y. Zhou, W. Ming, P. Yang, and J. Wu, "An overview of soft open points in electricity distribution networks," *IEEE Trans. Smart Grid*, vol. 13, no. 3, pp. 1899–1910, 2022.

[2] M. Deakin, I. Sarantakos, D. Greenwood, J. Bialek, P. C. Taylor, and S. Walker, "Comparative analysis of services from soft open points using cost–benefit analysis," *Appl. Energy*, vol. 333, no. October 2022, p. 120618, 2023.

[3] H. Ji, C. Wang, P. Li, F. Ding, and J. Wu, "Robust operation of soft open points in active distribution networks with high penetration of photovoltaic integration," *IEEE Trans. Sustain. Energy*, vol. 10, no. 1, pp. 280-289, 2019.

[4] P. Li, H. Ji, C. Wang, J. Zhao, G. Song, F. Ding, and J. Wu, "Optimal operation of soft open points in active distribution networks under three-phase unbalanced conditions," *IEEE Trans. Smart Grid*, vol. 10, no. 1, pp. 380–391, 2019.

[5] Q. Qi, J. Wu, and C. Long, "Multi-objective operation optimization of an electrical distribution network with soft open point," *Appl. Energy*, vol. 208, pp. 734–744, 2017.

[6] P. Li, H. Ji, C. Wang, J. Zhao, G. Song, F. Ding, and J. Wu, "Coordinated control method of voltage and reactive power for active distribution networks based on soft open point," *IEEE Trans. Sustain. Energy*, vol. 8, no. 4, pp. 1430–1442, 2017.

[7] I. Džafić, M. Gilles, R. A. Jabr, B. C. Pal, and S. Henselmeyer, "Real time estimation of loads in radial and unsymmetrical three-phase distribution networks," *IEEE Trans. Power Syst.*, vol. 28, no. 4, pp. 4839–4848, 2013.

[8] C. Long, J. Wu, L. Thomas, and N. Jenkins, "Optimal operation of soft open points in medium voltage electrical distribution networks with distributed generation," *Appl. Energy*, vol. 184, pp. 427–437, 2016.

[9] J. Zhao, M. Yao, H. Yu, G. Song, H. Ji, and P. Li, "Decentralized voltage control strategy of soft open points in active distribution networks based on sensitivity analysis," *Electronics*, vol. 9, no. 2, 2020.

[10] Z. Zhang, L. F. Ochoa, and G. Valverde, "A novel voltage sensitivity approach for the decentralized control of DG plants," *IEEE Trans. Power Syst.*, vol. 33, no. 2, pp. 1566-1576, 2018.

[11] P. Li, H. Ji, H. Yu, J. Zhao, C. Wang, G. Song, and J. Wu, "Combined decentralized and local voltage control strategy of soft open points in active distribution networks," *Appl. Energy*, vol. 241, no. March, pp. 613–624, 2019.

[12] L. Thomas, Y. Zhou, C. Long, J. Wu, and N. Jenkins, "A general form of smart contract for decentralized energy systems management," *Nat. Energy*, vol. 4, no. 2, pp. 140–149, 2019.

[13] Q. Qi, C. Long, J. Wu, and J. Yu, "Impacts of a medium voltage direct current link on the performance of electrical distribution networks," *Appl. Energy*, vol. 230, pp. 175–188, 2018.

[14] Y. Huo, P. Li, H. Ji, J. Yan, G. Song, J. Wu, and C. Wang, "Data-driven adaptive operation of soft open points in active distribution networks," *IEEE Trans. Ind. Informatics*, vol. 17, no. 12, pp. 8230–8242, 2021.

[15] E. Hnyilicza, S. T. Lee, and F. C. Schweppe, "Steady-state security regions: the set-theoretic approach," in *Proc. 1975 PICA Conf.*, 1975.

[16] F. F. Wu and S. Kumagai, "Steady-state security regions of power systems," *IEEE Trans. Circuits Syst.*, vol. 29, no. 11, pp. 703–711, 1982.

[17] T. Yang and Y. Yu, "Static voltage security region-based coordinated voltage control in smart distribution grids," *IEEE Trans. Smart Grid*, vol. 9, no. 6, pp. 5494–5502, 2018.

[18] T. Yang and Y. Yu, "Steady-state security region-based voltage/var optimization considering power injection uncertainties in distribution grids," *IEEE Trans. Smart Grid*, vol. 10, no. 3, pp. 2904–2911, 2019.

[19] X. Jiang, Y. Zhou, W. Ming, and J. Wu, "Feasible operation region of an electricity distribution network," *Appl. Energy*, vol. 331, no. July 2022, p. 120419, 2023.

[20] C. Liu, "A new method for the construction of maximal steady-state security regions of power systems," *IEEE Trans. Power Syst.*, vol. PWRS-1, no. 4, 1986.

[21] S. Wang, S. Chen, L. Ge, and L. Wu, "Distributed generation hosting capacity evaluation for distribution systems considering the robust optimal operation of OLTC and SVC," *IEEE Trans. Sustain. Energy*, vol. 7, no. 3, pp. 1111–1123, 2016.

[22] M. E. Baran and F. F. Wu, "Optimal capacitor placement on radial distribution systems," *IEEE Trans. Power Deliv.*, vol. 4, no. 1, pp. 725–734, 1989.

[23] IEEE, "IEEE 123-node test feeder," Sept. 29, 2024 [online]. https://cmte.ieee.org/pes-testfeeders/resources

[24] X. Cao, J. Wang and B. Zeng, "A study on the strong duality of second-order conic relaxation of ac optimal power flow in radial networks," *IEEE Trans. Power Syst.*, vol. 37, no. 1, pp. 443-455, 2022.

[25] L. Gan, N. Li, U. Topcu and S. Low, "Exact convex relaxation of optimal power flow in radial networks," *IEEE Trans. Autom. Control*, vol. 60, no. 1, pp. 72-87, 2015.



**Xun Jiang** (Member, IEEE) received the BSc and MSc degrees in electrical engineering from Tianjin University, Tianjin, China, in 2016 and 2019, respectively. He received the Ph.D. degree in electrical engineering from Cardiff University, U.K., in 2024. He is currently a Research Associate with the School of Engineering of Cardiff University, U.K. His research interests focus on smart electricity distribution networks and feasible operation region methodology.

**Yue Zhou** (Member, IEEE) received his B.Eng. and Ph.D. degrees in Electrical Engineering from Tianjin University, China, in 2011 and 2016, respectively. He is a Professor at the School of Electrical and Information Engineering, Tianjin University, China. He was a Postdoctoral Research Associate from 2017 to 2020 and became the Lecturer in Cyber Physical Systems in 2020, at School of Engineering, Cardiff University, Wales, UK. His research interests include demand response, electricity market, peer-to-peer energy trading and cyber physical systems.

**Jianzhong Wu** (Fellow, IEEE) received his BSc, MSc and Ph.D. degrees in Electrical Engineering from Tianjin University, China, in 1999, 2002 and 2004, respectively. From 2004 to 2006, he was at Tianjin University, where he was an Associate Professor. From 2006 to 2008, he was a Research Fellow at the University of Manchester, Manchester, U.K. He is a Professor of Multi-Vector Energy Systems and the Head of the School of Engineering, Cardiff University, U.K. His research interests include integrated multi-energy infrastructure and smart grid. He is Co-Editor-in Chief of Applied Energy. He is the Co-Director of U.K. Energy Research Centre and EPSRC Supergen Energy Networks Hub.

**Wenlong Ming** (Member, IEEE) received the B.Eng. and M.Eng. Degrees in Automation from Shandong University, Jinan, China, in 2007 and 2010, respectively. He received the Ph.D. degree in Automatic Control and Systems Engineering from the University of Sheffield, Sheffield, U.K., in 2015. He is the winner of the prestigious IET Control & Automation Doctoral Dissertation Prize in 2017. Since August 2020, he has been a Senior Lecturer of power electronics with Cardiff University, Cardiff, U.K., and since April 2020, he has been a Senior Research Fellow funded by Compound Semiconductor Applications Catapult, Newport, U.K., for 5 years. He was with the Center for Power Electronics Systems, Virginia Tech, Blacksburg, USA, in 2012, as an Academic Visiting Scholar. He has coauthored more than 60 papers published in leading journals or refereed IEEE conferences. His research interests include packaging, characterization, modelling, and applications of wide-bandgap semiconductor power devices.